Performance Analysis of IEEE 802.15.6 MAC Protocol under Non-Ideal Channel Conditions and Saturated Traffic Regime

Subhadeep Sarkar, *Student Member, IEEE*, Sudip Misra, *Senior Member, IEEE*, Bitan Bandyopadhyay, *Student Member, IEEE*, Chandan Chakraborty, and Mahammad S. Obaidat, *Fellow, IEEE*

Abstract—Recently, the IEEE 802.15.6 Task Group introduced a new wireless communication standard that provides a suitable framework specifically to support the requirements of wireless body area networks (WBANs). The standardization dictates the physical (PHY) layer and medium access control (MAC) layer protocols for WBAN-based communications. Unlike the pre-existing wireless communication standards, IEEE 802.15.6 standardization supports short-range, extremely low power wireless communication with high quality of service and support for high data rates upto 10 Mbps in the vicinity of living tissues. In this work, we construct a discrete-time Markov chain (DTMC) that efficiently depicts the states of an IEEE 802.15.6 CSMA/CA-based WBAN. Following this, we put forward a thorough analysis of the standard in terms of reliability, throughput, average delay, and power consumption. The work concerns non-ideal channel characteristics and a saturated network traffic regime. The major shortcoming of the existing literature on Markov chain-based analysis of IEEE 802.15.6 is that the authors did not take into consideration the time spent by a node awaiting the acknowledgement frame after transmission of a packet, until time-out occurs. Also, most of the work assume that ideal channel characteristics persist for the network which is hardly the case in practice. This work remains distinctive as we take into account the waiting time of a node after it transmits a packet while constructing the DTMC. Based on the DTMC, we perform a user priority (UP)-wise analysis, and justify the importance of the standard from a medical perspective.

Index Terms—IEEE 802.15.6, WBAN, discrete-time Markov model, user priorities, performance evaluation

1 Introduction

In the era of technology, the rise of embedded systems is redefining our standard of living, everyday. Wireless sensor networks (WSNs) have already found its wide-spread utilization in various application fields [1], [2], [3]. Healthcare has always been and still remains an area which lacks technological advancements. However, in recent times, healthcare systems have undergone a steep series of advancements. The use of WBANs in post-operative health monitoring and rehabilitation [4] has proven to be a great success in this reference. The traditional models for tele-monitoring, ambulatory care, tele-medicines systems, and distant and ubiquitous healthcare services [5], [6], [7], [8], [9] are re-defined in a different dimension with the introduction of WBANs. It can also be used to provide medical services in rural and remote areas, offering improved and cost-effective treatments, and, thereby, improving the quality of life. WBAN-based healthcare systems is considered to be highly efficient in constant and real-time monitoring of various physiological parameters of a patient, such as blood oxygen saturation level, glucose, pH, heart rate, and respiration rate. The system is also realized to be highly effective for the prevention and treatment of chronic diseases, such as asthma, diabetes, and cardiac diseases. Thus, the use of WBANs in modern healthcare systems has set about a new era in e-healthcare, making way to look beyond the traditional medical care systems.

A WBAN is a logical set comprising of multiple heterogeneous wireless body sensor nodes and a common hub [10], [11]. The sensor nodes in a WBAN are responsible for measuring certain physiological attributes of a person, constantly over time. The data sensed by these nodes are then broadcast over the wireless medium by the sensors to a common local hub, also known as local data processing unit (LDPU) [12]. The hub or LDPU, in turn, sends data via an access point (AP) to remote hospitals or medical care centers for their real-time analysis. In its initial stages, WBAN-communications primarily followed the IEEE 802.15.4 standardization [13]. The standard was originally designed to support wireless personal area networks (WPANs) operating on low data rates. The purpose of it

- *S. Sarkar is with the School of Information Technology and the School of Medical Science and Technology, Indian Institute of Technology, Kharagpur 721302, India. E-mail: subhadeep@smst.iitkgp.ernet.in.*
- *S. Misra is with the School of Information Technology, Indian Institute of Technology, Kharagpur 721302, India. E-mail: smisra@sit.iitkgp.ernet.in.*
- *B. Bandyopadhyay is with the Department of Electronics and Telecommunication Engineering, Jadavpur University, Kolkata 700032, India. E-mail: bitanbanerjee16@gmail.com.*
- *C. Chakraborty is with the School of Medical Science and Technology, Indian Institute of Technology, Kharagpur 721302, India. E-mail: chandanc@smst.iitkgp.ernet.in.*
- *M. S. Obaidat is with the Department of Computer Science and Software Engineering, Monmouth University, W. Long Branch, NJ. E-mail: obaidat@monmouth.edu.*

Manuscript received 15 Aug. 2014; revised 7 Dec. 2014; accepted 23 Dec. 2014. Date of publication 8 Jan. 2015; date of current version 10 Sept. 2015. Recommended for acceptance by H. Ammari.
For information on obtaining reprints of this article, please send e-mail to: reprints@ieee.org, and reference the Digital Object Identifier below.
Digital Object Identifier no. 10.1109/TC.2015.2389806

was to provide an efficient low-power and low-complexity, short-range radio frequency-based wireless communication standard with a support for node-mobility [14]. However, it was soon realized that the performance of the body sensor nodes operating on this IEEE 802.15.4 protocol is not satisfactory as the protocol does not support the improvement of quality of service (QoS) and increase of data rate. The recent standardization by the IEEE 802.15.6 Task Group provides a new set of PHY layer and MAC layer specifications [11], particularly for wireless communications involving WBANs. IEEE 802.15.6 is a standard for short range wireless communication in the vicinity of, or inside the human body, and it presents support for QoS, extremely low power, and high data rates up to 10 Mbps. It is complaint with the non-interference guidelines, and takes into account the mobility of the sensor nodes and radiation pattern shaping to minimize the specific absorption rate (SAR) into the human body. Apart from healthcare applications, the IEEE 802.15.6 standard supports different non-medical applications (e.g. video streaming, file transfer, and gaming) [15] as well. Therefore, it is very important to provide a complete and thorough analytical model for the IEEE 802.15.6 standard, in order to evaluate its network performance, and also to find possible improvements on the standard.

1.1 Motivation

Applications of WBANs span through diverse fields which includes distant and ubiquitous health monitoring, hospital and ambulatory healthcare, medical support in mass emergency situations, and nano-scale pervasive precision health monitoring and treatment actuation. Having mentioned the criticality and importance associated with its application domains, we highlight the importance of efficient modeling of the new communication standard. The DTMC-based modeling of the IEEE 802.15.6 CSMA/CA protocol assists in evaluation and comparison of the performance of the protocol against its previous counterparts. Additionally, it serves as a platform for future researches which would be conducted for the betterment of the protocol either through MAC sublayer modification or new algorithms to be run in the upper networking layers.

In the present literature, there are very few works [16], [17], [18], [19], [20], [21] that provide a generalized analytic model for the performance evaluation of the IEEE 802.15.6 standard. Inspired by Bianchi's works [22], [23] for IEEE 802.11 based networks, in this paper, we construct a DTMC that depicts the different states of an active body sensor node operating on the IEEE 802.15.6 protocol. In similar research works, which provide DTMC-based analysis of the IEEE 802.15.6 protocol, as in [16], [17], [18], [19], it is assumed that a node remains in the same state after the transmission of a packet, while waiting for the acknowledgement frame until the timer runs out. However, in practice, immediately after the transmission of a frame, the nodes start a counter, and increase its value after every time-slot. Therefore, it is important that the Markov model representing the different states of a node takes into consideration these states in order to accurately analyze the performance of the standard. A similar approach is adopted in [24] where we performed a theoretical analysis of the IEEE 802.15.6 CSMA/CA protocol for ideal channel conditions. This work, although, adheres the same underlying architecture and analytic model, remains distinctive, as it deals with the non-ideal channel properties. Based on the analysis, we derive the expressions for the different performance parameters under non-ideal channel properties, and compare those against the results obtained in [24].

Moreover, it is mention-worthy that none of the existing research works in this regard [20], [21] have considered all the necessary performance parameters, viz. reliability, throughput, average delay, and power consumption, together, to provide a rigorous performance analysis of the standard. Also, in the context of performance evaluation of IEEE 802.15.6, no work have considered reliability of the WBAN into account. Needless to mention, reliability is one of the crucial performance metrics for WBANs, as successful and timely delivery of health-data packets is highly important for ubiquitous and remote health monitoring. In this paper, based on the DTMC constructed, we formulate the expression for reliability, and, subsequently, model the expressions for throughput, average delay, and power consumption to provide a thorough analysis of the protocol.

1.2 Contribution

The main contributions of this article are summarized below.

- The analytical model is developed using a four dimensional Markov chain using user priority (UP), backoff stage, backoff counter, and re-transmission counter. We have also considered the collision detection process by uniquely modeling the acknowledgement receiving mechanism, and thus, calculated the probability of collision.
- We have evaluated all the necessary parameters for performance evaluation of the IEEE 802.15.6 standard, such as reliability, throughput, average delay, and power consumption. A thorough analysis of the standard based on the constructed DTMC provides a holistic analysis of the standard from a networking perspective.
- In this work, we also provide UP-based analysis of the standard, and examine the importance of the eight different user priorities which are introduced in the standard. Additionally, from a medical perspective, we critically comment on the impact of the user priority designated for medical applications, i.e., $UP(7)$.
- For performance evaluation we take account of non-ideal channel conditions by introducing BER, multipath fading, shadowing standard deviation, and error probability due to the modulation schemes, making our simulation results more comprehensive and close to practical performances.

1.3 Paper Organization

The rest of the paper is organized as follows. In Section 2 the existing works from related literature in this area are discussed. A brief overview of the IEEE 802.15.6 standard is provided in Section 3. In Section 4, we discuss the communication architecture of an IEEE 802.15.6 WBAN. The system

model depicting the different states of the IEEE 802.15.6 CSMA/CA access mechanism for the beacon enabled mode (Access mode 0) is described in Section 5. Also, in this Section, we obtain the expressions for reliability, throughput, and delay limits for a wireless body sensor node. We obtain the expressions for the different performance metrics in Section 6, and analyze the performance of the IEEE 802.15.6 standard based on the aforementioned attributes in Section 7. Finally, Section 8 concludes the analysis and discusses the future scope of work.

2 Related Work

In this paper, we construct a DTMC specifically to model the working of the IEEE 802.15.6 CSMA/CA access mechanism under saturation traffic and non-ideal channel conditions. There are several similar analytic studies, which are used to depict the working of different IEEE communication standards. Below, we classify the existing research works which are related to this paper into three major subheads.

2.1 DTMC-Based Analysis of Previous MAC Standards

The DTMC-based analyses of the different IEEE standards are mostly inspired by Bianchi's proposed model, which was introduced to analyze the IEEE 802.11 [25] distributed coordination function (DCF) [22], [23]. In [22] a DTMC-based analysis of the IEEE 802.11 standard under the saturated traffic regime is provided. The work was extended in [23], in which a thorough analysis of the DCF mechanism was given. In [26] the authors have provided an efficient algorithm for decreasing the backoff counter is proposed for the IEEE 802.11 standard which takes into consideration the anomalous slots.

Prior to the standardization of the IEEE 802.15.6 communication protocol, IEEE 802.15.4 was used in for wireless body sensor-based communications. There exists multiple DTMC-based analytical models for the performance evaluation of IEEE 802.15.4 protocol. Park et al. [27], and Marco et al. [28] modeled the states which a node may transit through after the transmission of a packet. The authors have introduced two different queues to model the waiting states of the transmitting node—one indicating the successful transmission of the packet, and the other representing the collision of the transmission of a packet. However, these works are done in context of the IEEE 802.15.4 standard, which is specified for low-rate wireless personal area networks (LR-WPANs).

2.2 DTMC-Based Analysis of IEEE 802.15.6

Although there exists few similar DTMC-based analytical works in the context of the IEEE 802.15.6 standard (e.g.: [16], [17], [18], [19]), none of these works provides a thorough performance analysis of the standard. Rashwand and Misic [16] and Rashwand et al. [17] provided a Markov chain-based analysis of the communication standard under non-saturation and saturation traffic conditions, respectively. In [18], some of the expected problems of the standard under saturation condition are discussed. The effects of the eight different access phases of the IEEE 802.15.6 is discussed in [19]. However, in these works, the authors have not taken into account the time spent by the sensor node waiting for an acknowledgement after it transmits a packet. It is assumed that the node retains its state for the entire duration until it receives an I-ACK frame from the LDPU, or the timer runs out indicating that the packet sent is dropped. On the contrary, in reality, a node starts off a counter immediately after it has transmitted the last bit of the data packet. The value of this counter is then increased linearly until the acknowledgement is received from the sender, or the maximum value for the counter ($mTimeout$) is reached.

However, from the modeling perspective, it is unclear that immediately after the transmission of a packet, how a node decides *a priori*, which of the two available queues it should enter. For a transmitting node, after the completion of the transmission of a packet, it simply waits for the I-ACK frame until timeout for the event to occur. During this wait, the node may not predict whether collision will take place or not. Arrival of the I-ACK frame remains a probabilistic event, depending on the channel conditions and the network traffic congestion. Therefore, it is impossible for a sensor node to select a waiting queue immediately after the transmission of a packet without having *a priori* knowledge about whether or not collision will take place for the transmitted packet. In this work, we design a DTMC that efficiently depicts all the states of the transmitting node. We introduce only a single queue which indicates the states of a node after the transmission of a packet. A node enters this queue following the successful transmission of a packet, and waits for the I-ACK frame to arrive until the timer runs out. We model the event of arrival of the I-ACK frame within $mTimeOut$ as a probabilistic one, and define the state transition probability accordingly.

2.3 Non-Markovian Analysis of IEEE 802.15.6

Ullah et al. [20], [21] provided non-Markovian analyses of the IEEE 802.15.6 standard in terms of throughput and delay limits. In these works, the authors derived the optimal network provisioning and packet lengths for different applications. However, the analyses were limited to ideal channel characteristics with packet transmission errors, and no user priority specific analysis were made in this reference. Tachtatzis et al. [29] performed energy analysis of the IEEE 802.15.6 scheduled access modes in the context of medical applications. The optimal superframe structure and the sleep duration of the nodes in terms of the number of superframes are calculated in these works in order to maximize the network lifetime. The analyses were performed on the draft version of the IEEE 802.15.6 standard, and these works do not put forward a complete performance evaluation of the standard.

In this work, we construct a DTMC to model the IEEE 802.15.6 CSMA/CA access mechanism for non-ideal channel conditions, and immediate acknowledge (I-ACK) policy. It may be noted at this juncture that the working of the IEEE 802.15.6 communication [11] protocol is significantly distinct from the previously known wireless communication standards [13], [25]. We consider saturated network traffic regime, and model the different states of a transmitting node along the time-axis, accordingly. Further, we use the

TABLE 1
Parameters and Traffic Designation for Different User Priorities

UP	CW_{min}	CW_{max}	Traffic designation
0	16	64	Background (BK)
1	16	32	Best effort (BE)
2	8	32	Excellent effort (EE)
3	8	16	Controlled load (CL)
4	4	16	Video (VI)
5	4	8	Voice (VO)
6	2	8	High priority medical data or Network control
7	1	4	Emergency or Medical implant event report

DTMC-based analysis to mathematically deduce the expressions for reliability, throughput, average delay, and power consumption of a WBAN node operating under the IEEE 802.15.6 series of protocols. Also, we provide thorough UP-based analyses of the standard, and compare and conclude over the importance the eight user priorities introduced in the standard.

3 Overview of IEEE 802.15.6

The IEEE 802.15.6 standard [11] is designed specifically to support communication in WBANs. It provides a set of guidelines for ultra-low power, short-range (within 10 m), and high data rates (up to 10 Mbps) wireless communication in the vicinity of, or within the human body. It also proposes strict non-interference guidelines with support for improved QoS and reliability. The standard takes into consideration the effects on the micro-antennas within the sensor nodes due to the presence of living beings with varied height, weight, and gender, the motion of the users, and shaping of the radiation pattern to minimize the specific absorption rate. In this Section, a brief outline of the PHY and the MAC layers for the IEEE 802.15.6 standard is provided.

A major modification that was introduced in the standard is the introduction of eight different user-priorities based on the traffic designation. The values of the minimum and maximum sizes of the contention window changes along with the traffic designation are depicted in Table 1.

3.1 PHY Layer Specifications

The 802.15.6 standard supports three PHY, Narrowband (NB), Ultra Wideband (UWB) and Human Body Communications (HBC) [11], [30]. The main features of the different PHY layers are mentioned below.

3.1.1 Narrowband PHY

The NB PHY is an optional physical layer, which is responsible for the following tasks:

- Activation and deactivation of the radio transceiver.
- Clear channel assessment (CCA).
- Data transmission and reception [11].

The PHY layer supports different frequency bands—402-405, 420-450, 863-870, 902-928, 950-958, 2,360 to 2,400, and 2,400-2,483.5 MHz [31].

3.1.2 Ultra Wideband PHY

The Ultra Wideband PHY is used to provide a data interface to the MAC layer under the control of Physical Layer Convergence Protocol (PLCP). Its main functions are:

- Activation and deactivation of the radio transceiver.
- The PLCP constructs the PHY layer protocol data unit (PPDU) by concatenating the synchronization header (SHR), physical layer header (PHR) and physical layer service data unit (PSDU), respectively.
- It may provide CCA indication to the MAC [11].

3.1.3 Human Body Communications PHY

Human Body Communication PHY supports two modes of operation—default mode and high quality of service mode, depending on the application. HBC PHY operates in two frequency bands centred 16 and 27 MHz with the bandwidth of 4 MHz. The main operation of HBC is to provide electrostatic field communication (EFC) specification for the whole WBAN.

According to the standard, a maximum of 64 nodes may be connected to a hub or LDPU simultaneously. Also, it is mentioned that a WBAN operating according to the IEEE 802.15.6 communication guidelines, can operate in one of the three access modes as explained in Section 3.2.

3.2 MAC Layer Specifications

3.2.1 Beacon Enabled Access Mode 0

In this mode the nodes are synchronized by periodic transmission of the beacon (superframe) from the hub. Every superframe includes Exclusive Access Phase 1 (EAP1), Random Access Phase 1 (RAP1), Type I/II phase, Exclusive Access Phase 2 (EAP2), Random Access Phase 2 (RAP2), another Type I/II phase, Managed Access Phase (MAP), and Contention Access Phase (CAP). The EAP1 and EAP2 are used in highest user priority, and the RAP1, RAP2 and CAP are used for other traffic conditions.

3.2.2 Non-Beacon Access Mode 0

In this access mode, the whole superframe duration is allocated by either Type I/II phases, but not by both.

3.2.3 Non-Beacon Access Mode 1

Access Mode 1 is the non-beacon mode without superframe. In this mode, the hub grants unscheduled Type II polled allocation, which allows the sensor to transmit only a limited number of frames.

Another crucial modification that is introduced in the IEEE 802.15.6 standard is in regards the updation of the value of the backoff counter for a node. For a node operating in $UP(i)$, the value of the backoff counter is initialized to a randomly chosen integer over $[1, W_0^i]$, where W_0^i denotes the minimum value of the backoff counter for a node operating in $UP(i)$. Following this, for every odd number of retry, the value of the contention window is left unaltered. On the contrary, for every even number of retries, the value is doubled. This procedure is continued until the value of the contention window reaches or exceeds its maximum value for that user priority. In such

cases, the contention window value is set to W^i_{max}, as per Table 1. Mathematically,

$$W^i_k = \begin{cases} W^i_0, & \text{when } k = 0, \\ W^{i-1}_k, & \text{when } l \text{ is odd}, 1 \leq k \leq m, \\ min\{2W^{i-1}_k, W^i_{max}\}, & \text{when } l \text{ is even}, 2 \leq k \leq m, \end{cases} \quad (1)$$

where, l corresponds to the number of re-transmissions that a data-packet has underwent.

The IEEE 802.15.6 standard also uses the backoff freezing mechanism during data transmission(see Fig. 1). A node freezes or locks its backoff counter, if any one of the following events occurs:

- The backoff counter is reset upon decrementing to zero.
- The channel is sensed busy due to the transmission of a frame by any other sensor node of the network. In such a case, the channel remains busy at least until the end of the current frame transmission.
- The current time is outside any RAP or CAP for $UP(i)$ where $i \in (0, 6)$, or is outside any EAP, RAP, or CAP for $UP(7)$.
- Although the current time is the beginning of a CSMA slot and within the EAP, RAP, or CAP, the time remaining between the end of the present slot and the end of the EAP, RAP, or CAP is insufficient for the completion of frame transmission.

A frozen or locked backoff counter, however, is unlocked by the node, if both the following conditions are satisfied concurrently.

- The channel is sensed idle by the node for $pSIFS$ duration during the RAP or CAP for $UP(i)$, where $i \in (0, 6)$, or during the EAP, RAP, or CAP for $UP(7)$.
- The remaining time between the current time plus a CSMA slot and the end of the EAP, RAP, or CAP is long enough to transmit the next frame in its entirety.

The beacon superframe structure is divided into subgroups of different access phases. This phases are named as EAP1, EAP2, RAP1, RAP2, MAP, and CAP. Each beacon period is composed of s ($s \leq 256$) number of allocation slots of equal length. The length of different access phases are defined by the MAC header of the current beacon frame. Data frame transmission takes place only during the contended allocations in EAP1, EAP2, RAP1, RAP2, and CAP.

EAP. EAP is a time period in the beacon-enabled superframe structure used by sensor of highest priority for the purpose of data transfer. For highest priority sensors, EAP1 and RAP1 are combined to form EAP1, and EAP2 and RAP2 are combined to form EAP2 for continuous data transmission and better channel utilization, which, in turn, improves the throughput of the system too. If EAP1 has a nonzero length, it starts immediately after the preceding beacon. The length of EAP1 and EAP2 are defined using the EAP indicator field and connection assignment frame, respectively.

RAP. RAP is an allocation period which is used for data transmission. However, in contrary to EAP, in RAP only nodes transmitting data packets of regular priority are allowed to transmit. Sensor nodes, which transmit data of highest priority (operating in $UP(7)$) are forbidden to transmit during this access phase. There exists few similarities between EAP and RAP, such as both can have zero length, which is determined by the MAC header. Moreover, EAP and RAP are present in the current beacon period, if beacon shifting is not enabled in the present beacon period. The RAP1 start field is mentioned only when the EAP1 has a nonzero length, as indicated by the EAP indicator field in the MAC header. If EAP1 is absent, then RAP1 starts immediately after the preceding beacon. Similar process takes place for defining the RAP2 start, which depends on the length of EAP2.

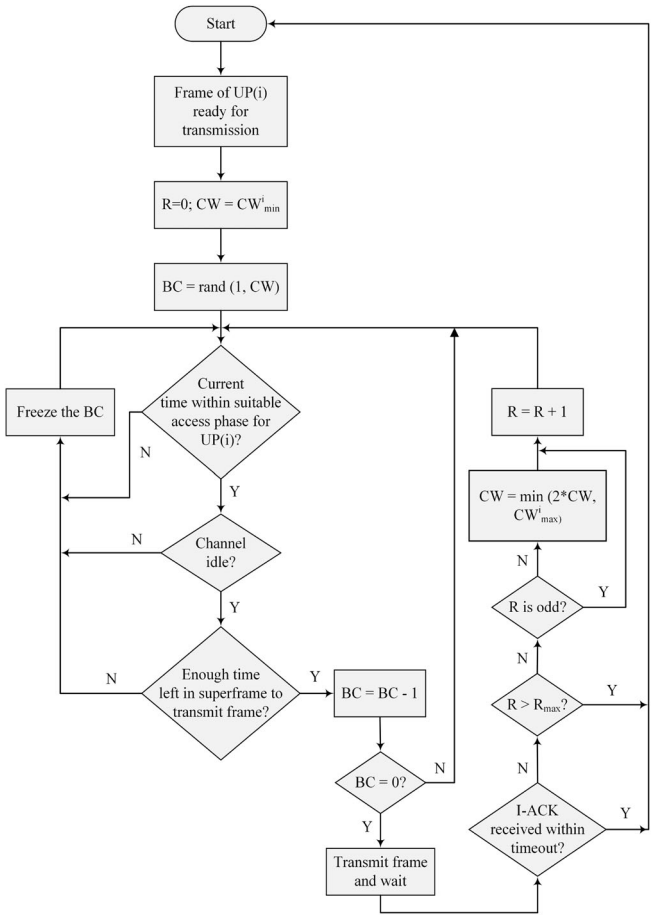

Fig. 1. IEEE 802.15.6 CSMA/CA.

CAP. CAP is the phase used for uplink frame transition, similar to EAP and RAP. For nonzero length of CAP, a B2 frame is transmitted and CAP starts immediately after the end of the B2 frame. The length of CAP is defined as the allocation slots between the endings of B2 frame and the present beacon period.

MAP. MAP differs from the previously mentioned access phases. Only during MAP, a hub can arrange scheduled uplink, downlink or bilink allocation intervals, provide unscheduled bilink intervals and improvise type-I, immediate polled allocation intervals and posted allocation intervals starting from this MAP. During a MAP, a sensor, however, may be in inactive state.

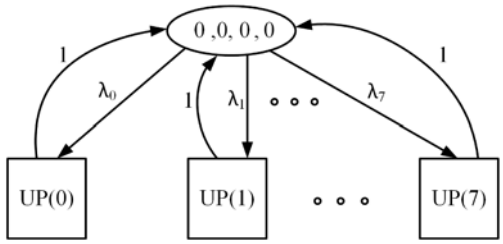

Fig. 2. DTMC considering all UPs of IEEE 802.15.6 CSMA/CA.

4 Communication Architecture

In this section, we describe the generalized communication architecture and the heterogeneous network topology for WBANs. The communication architecture for WBANs may be divided into three sub-parts—*intra-BAN* communications, *inter-BAN* communications, and *beyond-BAN* communications [10]. However, intra-BAN communication aspects involving the wireless hub (or LDPU) and the connected wireless body sensor nodes are the major areas of focus of the IEEE 802.15.6 standard. A WBAN may consist of only one hub, and up to $mMaxBANSize$ ($mMaxBANSize$ is often set to 64) number of sensor nodes connected to it. The sensor nodes are connected to the hub, over the wireless medium, in a star network topology. The standard supports both one-hop and two-hop communications for the WBANs.

In this paper, we consider single-hop wireless communication with the body sensor nodes connected with the hub to form a star network topology. The number of nodes connected to the hub in the one-hop star WBAN is n ($n \leq mMaxBANSize$). Although the mechanisms for coexistence and interference mitigation between adjacent or overlapping WBANs are provided in the standard, it does not provide any mechanism to establish coordination between different adjusting WBANs for the medium access at the MAC sub-layer. Our work provides a thorough performance analysis for such a WBAN working under the IEEE 802.15.6 CSMA/CA protocol.

5 System Model

In this Section, we design a DTMC that accurately depicts the different states involved in the CSMA/CA access mechanism for beacon enabled (Access Mode 0) IEEE 802.15.6 with finite retry limits. We assume a single hop, star topology for the network which consists of n_i number of body sensor nodes connected to a single sink for $UP(i)$. Clearly, $\sum_i n_i = n \leq mMaxBANSize$. The system is modeled for *saturated traffic regime* with non-ideal channel conditions, and for the immediate acknowledgement policy. Also, it is assumed that the collision probability of a packet transmitted by a station is invariant of the number of re-transmissions [22], [23] already suffered by it. We adopt the same analytic model as presented in [24] to obtain the equations for the normalization condition. Following this, we develop the expressions for the different performance metrics for non-ideal channel conditions in Section 6, and compare the results against that for the ideal channel properties in Section 7.

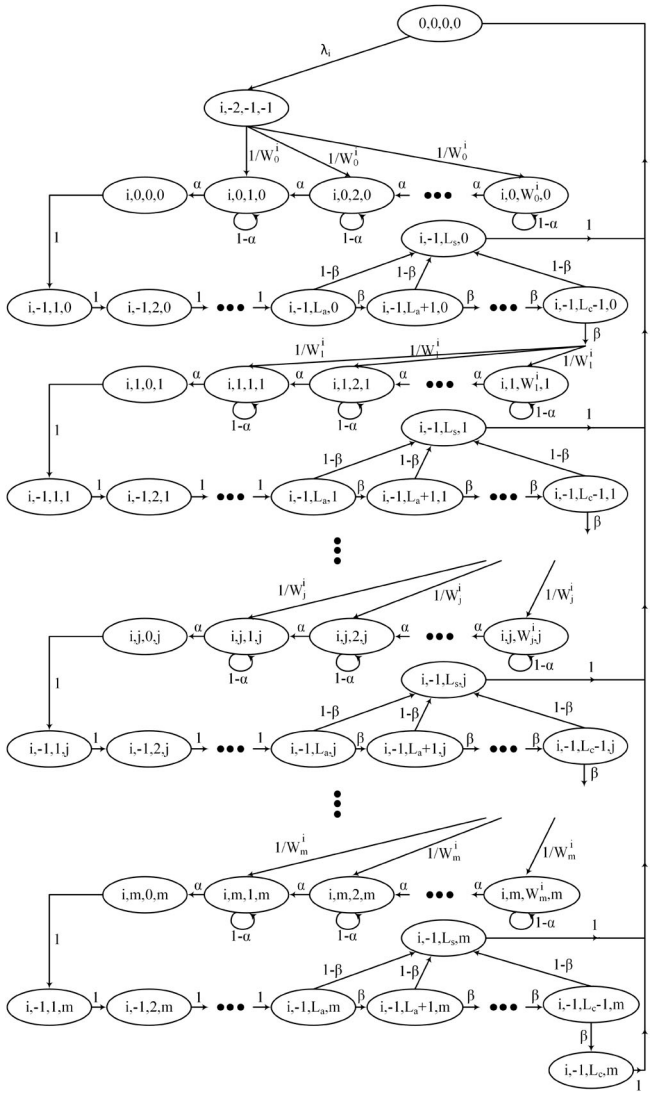

Fig. 3. DTMC for $UP(i)$ in IEEE 802.15.6 CSMA/CA.

5.1 Markov Chain

The DTMC is constructed as a four-tuple $u(t), s(t), b(t), r(t)$. The stochastic processes $u(t)$, $s(t)$, $b(t)$, and $r(t)$ represent the user priority to which a node belongs, the backoff stage, the backoff counter, and the re-transmission counter at time t, respectively. In Fig. 2, we draw a Markov model that considers all the eight user priorities ($UP(0)$ to $UP(7)$) supported by the IEEE 802.15.6 CSMA/CA access mechanism. The UPs are represented as blocks in this figure, and the states and the corresponding transitions are kept abstracted.

The internal structure of one of these blocks ($UP(i)$) is shown in detail in Fig. 3. The analysis based on this Markov chain is divided into two parts. First, we obtain the expressions for all the states in the Markov chain in terms of the initial state, i.e., $(0, 0, 0, 0)$ using chain regularities, and, finally, we compute the value of $b_{0,0,0,0}$ using the normalization condition. In the second part, we compute the expressions for reliability, throughput, average delay, and power consumption, and analyze the performance of the standard.

For any transmitting node, whenever it has a packet to send, it selects $UP(i)$ with probability λ_i, as shown in Fig. 2.

Clearly, $\sum_{i=0}^{7} \lambda_i = 1$. The node, then, chooses a random value over the interval $[1, W_0^i]$ against its backoff counter. W_0^i denotes the value of CW_{min} for a node operating in $UP(i)$ (see Table 1). Initially, the values for the backoff stage and the re-transmission counter are set to zero. The queue of states, from (i, j, W_j^i, l) to $(i, j, 1, l)$ denotes the phenomenon of backoff counter decrement for the jth backoff stage. Locking and unlocking of backoff counters are determined by simultaneous condition satisfactions, as mentioned in Section 3. A node transmits a packet immediately after its backoff counter reaches zero, i.e., after it reaches the $(i, j, 0, l)$ state.

After transmitting a packet, the value for the backoff stage of the node is set to -1, and a counter is started by the node. At this point, the re-transmission counter (which is the fourth tuple) acts as representative of the backoff stage. As depicted in Fig. 3, the queue of states, from $(i, -1, 1, l)$ to $(i, -1, L_c - 1, l)$, through $(i, -1, L_a - 1, l)$ represents the wait duration of a node for the lth (re)transmission. The value of this counter is incremented by unity after every timeslot, until the timer for the I-ACK reception (L_c) runs out. L_a denotes the minimum time required for the I-ACK frame to be received. After this time interval, if the packet delivery is successful, and the corresponding I-ACK frame is received, the node reaches the $(i, -1, L_s, l)$ state. Otherwise, it continues to increase the re-transmission counter until it reaches $(L_c - 1)$. At this stage, if the awaited I-ACK frame is still not received, the node moves on to the next backoff stage, and the value of its re-transmission counter is incremented by unity. The value of the backoff counter is updated as per Equation (1), depending on the number of retries the packet underwent. This procedure continues until the re-transmission limit is reached, and the time-out for I-ACK reception occurs. At this point, the node drops the packet, and returns to its initial state, $(0, 0, 0, 0)$. The one-step, non-null probabilities for the DTMC, as shown in Fig. 3, are:

$$P\{(i, -2, -1, -1)|(0, 0, 0, 0)\} = \lambda_i, \quad \text{for } i \in (0, 7), \tag{2}$$

$$P\{(i, 0, k, 0)|(i, -2, -1, -1)\} = \frac{1}{W_0^i}, \quad \text{for } k \in \left(0, W_0^i\right), \tag{3}$$

$$P\{(i, j, k, l)|(i, j, k+1, l)\} = \alpha, \quad \text{for } j \in (0, m), k \in \left(0, W_l^i - 1\right), l = j, \tag{4}$$

$$P\{(i, j, k, l)|(i, j, k, l)\} = 1 - \alpha, \quad \text{for } j \in (0, m), k \in \left(1, W_l^i\right), l = j, \tag{5}$$

$$P\{(i, -1, 1, l)|(i, j, 0, l)\} = 1, \text{ for } j \in (0, m), l = j, \tag{6}$$

$$P\{(i, -1, k+1, l)|(i, -1, k, l)\} = 1, \quad \text{for } k \in (1, L_a - 1), l \in (0, m), \tag{7}$$

$$P\{(i, -1, k+1, l)|(i, -1, k, l)\} = \beta, \quad \text{for } k \in (L_a, L_c - 2), l \in (0, m), \tag{8}$$

$$P\{(i, -1, L_s, l)|(i, -1, k, l)\} = 1 - \beta, \quad \text{for } k \in (L_a, L_c - 1), l \in (0, m), \tag{9}$$

$$P\{(i, j, k, l)|(i, -1, L_c - 1, l-1)\} = \frac{\beta}{W_l^i}, \quad \text{for } j \in (1, m), k \in \left(1, W_l^i\right), l = j, \tag{10}$$

$$P\{(i, -1, L_c, m)|(i, -1, L_c - 1, m)\} = \beta, \tag{11}$$

$$P\{(0, 0, 0, 0)|(i, -1, L_s, l)\} = 1, l \in (0, m), \tag{12}$$

$$P\{(0, 0, 0, 0)|(i, -1, L_c, m)\} = 1. \tag{13}$$

Equation (2) denotes the probability with which a node chooses to operate in $UP(i)$ after it has a data packet with ith user priority ready to be transmitted. The backoff counter is randomly set to a value ranging from $[1, CW]$, and is expressed in Equation (3). Equation (4) denotes the probability of idle channel and there is enough time in the present access period for data packet transmission. Similarly, Equation (5) represents the probability that the channel is busy or there is not enough time for data transmission. Equations (6) and (7) define that the data packet transmission is started and the data transmission is going on, respectively. The probability that the I-ACK frame is not received after completion of data packet transmission is denoted by Equation (8), and the value of counter increases. The probability of I-ACK reception, and, hence, concluding successful data transmission is denoted by Equation (9). The probability of unsuccessful data transmission and random selection of the value of the backoff counter is given in Equation (10). From the final state, to determine the unsuccessful data delivery, and again to set the backoff counter randomly, Equation (11) is used. Equations (12) and (13) represent the transition of a node to the initial state after successful and unsuccessful transmission of a data packet, respectively.

Our objective is to find the stationary probability for each state, and, thus, to compute the expressions for reliability and throughput of a node. Let the stationary distribution of the Markov chain be, $b_{i,j,k,l} = \lim_{t\to\infty} P\{u(t) = i, s(t) = j, b(t) = k, r(t) = l\}, i \in (0, 7), j \in (-2, m), k \in (-1, max(W_l^i, L_s, L_c)), l \in (-1, m)$. We now obtain the closed-form solution for this DTMC using chain regularities.

From Equations (4), (5), and (10), we get:

$$b_{i,j,k,l} = \frac{W_l^i - k + 1}{\alpha W_l^i} \beta^{(L_c - L_a)l} \times b_{i,0,0,0}, \quad \text{where } j \in (0, m), k \in \left(1, W_l^i\right), l = j. \tag{14}$$

Equation (9) through (10), and (14) yield:

$$b_{i,j,0,l} = \beta^{(L_c - L_a)l} \times b_{i,0,0,0}, \quad \text{where } j \in (0, m), l = j, \tag{15}$$

$$b_{i,0,k,0} = \frac{W_0^i - k + 1}{\alpha W_0^i} \times b_{i,0,0,0}, \quad \text{where } k \in \left(1, W_0^i\right). \tag{16}$$

Also, we get:

$$b_{i,-1,k,l} = \begin{cases} b_{i,j,0,l}, & j \in (0, m), k \in (1, L_a - 1), j = l, \\ \beta^{k - L_a} b_{i,j,0,l}, & j \in (0, m), k \in (L_a, L_c - 1), j = l. \end{cases} \tag{17}$$

From Equations (10) and (17), we have:

$$b_{i,-1,L_c-1,l} = \beta^{(L_c-L_a-1)+(L_c-L_a)l} \times b_{i,0,0,0}, \quad \text{where } l \in (0,m). \tag{18}$$

Finally, from Equation (12), we get:

$$b_{i,-1,L_s,l} = (1-\beta^{L_c-L_a}) \times b_{i,j,0,l}, \text{ where } l \in (0,m), j = l. \tag{19}$$

By imposing the normalization condition, we get:

$$1 = \sum_{i=0}^{7}\sum_{j=0}^{m}\sum_{k=0}^{W_j^i} b_{i,j,k,l} + \sum_{i=0}^{7}\sum_{k=1}^{L_c-1}\sum_{l=0}^{m} b_{i,-1,k,l} + \sum_{i=0}^{7}\sum_{l=0}^{m} b_{i,-1,L_s,l} + \sum_{i=0}^{7} b_{i,-1,L_c,m} \tag{20}$$

$$+ \sum_{i=0}^{7} b_{i,-2,-1,-1} + b_{0,0,0,0.} \tag{21}$$

We now derive each of the terms in Equation (20) separately

$$\sum_{i=0}^{7}\sum_{j=0}^{m}\sum_{k=0}^{W_j^i} b_{i,j,k,l} = \sum_{i=0}^{7}\sum_{j=1}^{m}\sum_{k=1}^{W_j^i} b_{i,j,k,l} + \sum_{i=0}^{7}\sum_{j=1}^{m} b_{i,j,0,l} + \sum_{i=0}^{7}\sum_{k=1}^{W_0^i} b_{i,0,k,0} + \sum_{i=0}^{7} b_{i,0,0,0.} \tag{22}$$

We compute the first part of Equation (22) as given by Equation (22), where

$$\Psi = W_0^1\lambda_1 + W_0^2\lambda_2 + \cdots + W_0^7\lambda_7,$$

$$\sum_{i=0}^{7}\sum_{j=1}^{m}\sum_{k=1}^{W_j^i} b_{i,j,k,l} = \begin{cases} \frac{\beta^{L_c-L_a}}{2\alpha}\left[\left(\frac{1-\beta^{m(L_c-L_a)}}{1-\beta^{L_c-L_a}}\right) + \frac{1}{1-2\beta^{2(L_c-L_a)}} (1-(2\beta^{2(L_c-L_a)})^{m/2})(1+2\beta^{L_c-L_a})\Psi\right] \times b_{0,0,0,0} & \text{if m is even} \\ \frac{\beta^{L_c-L_a}}{2\alpha}\left[\left(\frac{1-\beta^{m(L_c-L_a)}}{1-\beta^{L_c-L_a}}\right) + \frac{2\beta^{L_c-L_a}}{1-2\beta^{2(L_c-L_a)}} (2-(2\beta^{2(L_c-L_a)})^{(m-1)/2})(1+2\beta^{2(L_c-L_a)})\Psi\right] \times b_{0,0,0,0} & \text{otherwise.} \end{cases} \tag{23}$$

The remaining terms of Equation (22) are computed as follows:

$$\sum_{i=0}^{7}\sum_{j=1}^{m} b_{i,j,0,l} = \beta^{L_c-L_a}\frac{1-\beta^{m(L_c-L_a)}}{1-\beta^{L_c-L_a}} \times b_{0,0,0,0,} \tag{24}$$

$$\sum_{i=0}^{7}\sum_{k=1}^{W_0^i} b_{i,0,k,0} = \frac{1+\Psi}{2\alpha} \times b_{0,0,0,0,} \tag{25}$$

$$\sum_{i=0}^{7} b_{i,0,0,0} = \sum_{i=0}^{7} \lambda_i b_{0,0,0,0} = b_{0,0,0,0.} \tag{26}$$

By substituting the values obtained from Equations (22), (24), (25), and (26) in (22), we get the expression for $\sum_{j=0}^{m}\sum_{k=0}^{W_j^i} b_{i,j,k,l}$

$$\sum_{i=0}^{7}\sum_{k=1}^{L_c-1}\sum_{l=0}^{m} b_{i,-1,k,l} = (1-\beta^{(m+1)(L_c-L_a)}) \left[\frac{(L_a-1)}{1-\beta^{L_c-L_a}} + \frac{1}{1-\beta}\right] \times b_{0,0,0,0}, \tag{27}$$

$$\sum_{i=0}^{7}\sum_{l=0}^{m} b_{i,-1,L_s,l} = \left[1-\beta^{(m+1)(L_c-L_a)}\right] \times b_{0,0,0,0}, \tag{28}$$

$$\sum_{i=0}^{7} b_{i,-1,L_c,m} = \beta^{(m+1)(L_c-L_a)} \times b_{0,0,0,0}, \tag{29}$$

$$\sum_{i=0}^{7} b_{i,-2,-1,-1} = b_{0,0,0,0}. \tag{30}$$

Equations (22), (27), (28), and (29) yield the values of the states as a function of $b_{0,0,0,0}$. Substituting the values obtained from these equations in Equation (20), we get the value of $b_{0,0,0,0}$

$$b_{0,0,0,0} = \begin{cases} \left[\left(\frac{\beta^{L_c-L_a}}{2\alpha}+L_a\right)\left(\frac{1}{1-\beta^{L_c-L_a}}\right) + \frac{1}{1-\beta} + \frac{1+\Psi}{2\alpha} + \frac{\Psi\beta^{L_c-L_a}}{\alpha(1-2\beta^{2(L_c-L_a)})} + 3\right]^{-1}, & \text{if } m \text{ is even,} \\ \left[\left(\frac{\beta^{L_c-L_a}}{2\alpha}+L_a\right)\left(\frac{1}{1-\beta^{L_c-L_a}}\right) + \frac{1}{1-\beta} + \frac{1+\Psi}{2\alpha} + \frac{2\Psi\beta^{2(L_c-L_a)}}{\alpha(1-2\beta^{2(L_c-L_a)})} + 3\right]^{-1}, & \text{otherwise.} \end{cases} \tag{31}$$

5.2 Non-Ideal Channel Characteristics

Under non-ideal channel conditions, wireless communication is affected by several factors, which result in the degradation of signal quality, and bit-level errors. Two such factors which cause such disputes in a wireless communication network are multipath fading and channel interference.

Multipath fading is the process in which transmitted signal reaches the destination through various propagation paths. Hence, fluctuations in amplitude and phase of the transmitted signal take place. In the presence of strong line of sight (LOS) propagation, we may ignore the fading effect, but in WBANs, multipath fading must be taken into consideration, as modelling the antenna supporting LOS propagation is a challenging issue in WBANs. Depending on the spatial parameters and mobility of the transmitter and receiver, multipath fading can be classified into two categories—small-scale fading and large-scale fading. For WBANs, the latter one is experienced mainly, as the distance between transmitter and receiver is small. Generally there is no shadowing effect by large obstructions too. Therefore, we can ignore the large-scale fading effect. To

model this kind of non-LOS propagation channels, especially for WBANs, Lognormal distribution or Rician distribution is followed. For modeling the error prone channel, we also need to consider co-channel interference caused by the crosstalk of two different transmitter, a matter of concern in WBANs, as there are number of on-body sensor in any WBANs. Average bit error rate (BER) or symbol error rate (SER) must be taken into account too, for performance evaluation. From the BER or SER in physical layer parameters and modulation processes, we evaluate the resulting packet error rate (PER).

According to the IEEE 802.15.6 standard, for the 2,360-2,400 and 2,400-2,483.5 MHz bands, the supported modulation schemes are DBPSK and DQPSK, respectively. For modeling error channel for this standard, the fading channel must be in the form of multiplicative distortion with additive white Gaussian noise (AWGN) channel. The capacity of AWGN and fading channels is calculated from its available transmit power and bandwidth. If the instantaneous signal-to-noise ratio (SNR) of the channel is denoted by γ, then transmit power can also be expressed as $\Delta(\gamma)$, hence the average transmit power can be equated as,

$$\int_0^\infty \Delta(\gamma)\nabla(\gamma)d\gamma \leq \bar{\Delta}, \tag{32}$$

where $\bar{\Delta}$ and $\nabla(\gamma)$ denotes average SNR and a function depending upon the distribution (Rician or Lognormal) followed by the propagation channel. For calculating BER or PER, we first need to obtain the conditional error probability (CEP), $P_e(\gamma)$. The average BER ($\overline{P_e}$) is calculated as:

$$\overline{P_e} = \int_0^\infty P_e(\gamma)\nabla(\gamma)d\gamma. \tag{33}$$

For DBPSK and DQPSK, $P_e(\gamma)$ is expressed as respectively,

$$P_e(\gamma)_{DBPSK} = ae^{-b\gamma}, \tag{34}$$

where $a = 0.5$ and $b = 1$.

$$P_e(\gamma)_{DQPSK} = Q(a\sqrt{\gamma}, b\sqrt{\gamma}) - \frac{1}{2}I_0(ab\gamma)e^{-\frac{a^2+b^2}{2}\gamma}, \tag{35}$$

where $a = \sqrt{2-\sqrt{2}}$,$b = \sqrt{2+\sqrt{2}}$ and $Q()$ is the Marcum Q-function and I_0 is a infinite series function, which can be expressed as,

$$I_r(x) = \left(\frac{1}{2}x\right)^r \sum_0^\infty \frac{\left(\frac{1}{4}x^2\right)^k}{k!\Gamma(v+k+1)}, \tag{36}$$

where, v is a integer obtained from the basic equation of Bessel function,

$$x^2\frac{d^2w}{dx^2} + x\frac{dw}{dx} + (x^2 - v^2)w = 0. \tag{37}$$

Now replacing $P_e(\gamma)$ in Equations (34) and (35), we obtain the average BER for DBPSK and DQPSK.

Again, for computation of blocking probability under the non-ideal channel conditions, we assume that the total number of available channels and total number of sensor nodes present in the system to be C and n, respectively. We consider the scenario, where $N(N \leq n \leq mMaxBANSize)$ sensor nodes attempt to access a single channel (any one of the C available channels). Among these N sensor nodes, if κ number sensors were already accessing the channel with $N - \kappa$ new attempts, the average channel access attempt rate (Λ) is:

$$\Lambda = (N - \kappa)\Lambda. \tag{38}$$

Therefore, the corresponding blocking probability P_{bl} is expressed as:

$$P_{bl} = \frac{{}^XC_N\left(\frac{\Lambda}{T_{pr}}\right)^N}{\sum_{i=0}^N {}^XC_i\left(\frac{\Lambda}{T_{pr}}\right)^i}, \tag{39}$$

where T_{pr} is the frame processing time at the receiver (hub)-end. However, as the number of available channels in IEEE 802.15.6 quite high (varies between 10 and 79 for different frequency bands) compared to the number of sensor nodes present in the system ($\leq$64, typically between 5 and 15), the value of Λ is observed to be very low, which, in turn, yields a negligible magnitude of P_{bl}.

5.3 Failure Probability

Failure probability, in the context of packet transmission, is defined as the probability with which a packet gets dropped during its transportation, i.e., it fails to reach the intended recipient successfully. In this case, we consider the collision probability and the inherent packet drop probability due to non-ideal channel properties into account as the principle reasons behind packet drops. Mathematically, failure probability (P_f) is expressed as:

$$P_f = 1 - \left(P_c^i \cap P_{pe}\right), \tag{40}$$

where P_c^i denotes the collision probability for a data packet transmitted by a node of $UP(i)$, and P_{pe} is the corresponding packet error probability.

Packet error probability PER is calculated from the BER using the following equation,

$$P_{pe} = 1 - (1 - P_e)^N, \tag{41}$$

where N is the bit length of the packet.

We now compute the collision probability (P_c^i) of a packet transmitted by a node that is operating in $UP(i)$. It might be reiterated that P_c^i is independent of the number of re-transmissions the packet has already undergone. For this, we first compute τ_i, the transmission probability for a node operating in $UP(i)$, given that the channel is idle at the time of the transmission. Clearly,

$$\begin{aligned}\tau_i &= \sum_{l=0}^m b_{i,j,0,l}, \qquad \text{where } j = l \\ &= \frac{1 - \beta^{(m+1)(L_c - L_a)}}{1 - \beta^{L_c - L_a}} \times b_{i,0,0,0}.\end{aligned} \tag{42}$$

Therefore, P_c^i is mathematically expressed as:

$$P_c^i = 1 - \left[\prod_{j=0}^7 (1-\tau_j)^{n_j} + (1-\tau_i)^{n_i - 1}\prod_{j=0, j\neq i}^7 (1-\tau_j)^{n_j}\right], \tag{43}$$

TABLE 2
Notations and Descriptions

Parameters	Values
Maximum CSMA Backoffs	8
Payload size	0-255 Bytes
Symbol rate	600 ksps
Unit Slot length	75 μs
Short interframe spacing (pSIFS)	75 μs
Extra interframe spacing (pExtraIFS)	10 μs
Acknowledgement wait duration	30 μs
Header size	32/symbol rate
E_{idle}	267 μW
E_{tx}	414 μW
E_{rx}	393 μW

where, n_i is the number of nodes operating under $UP(i)$, and are connected to the hub or LDPU. Clearly, for a system with a total of n number of nodes, $\sum_{i=0}^{7} n_i = n$.

Note that following a failed transmission of a data packet, a node should wait a time duration between $pSIFS$ and $pSIFS + pExtraIFS$ before the commencement of the retransmission of that frame [11]. Therefore, the recovery time for a node is expressed as: $(2 \times pSIFS + pExtraIFS)/2$. However, for the hub, after the reception of a data frame, it has to wait for a duration between $pMIFS$ and $pMIFS + pExtraIFS$ duration before transmitting the I-ACK, where $pMIFS$ demotes the minimum interframe spacing time.

6 Performance Metrics

In this section, we obtain the expressions for the principal performance metrics, viz. reliability, throughput, delay, and power consumption.

6.1 Reliability

We define *reliability* ($\mathcal{R}$) of a node as the probability of successful delivery of a transmitted packet. In other words, it is the complementary probability with which a transmitted packet is dropped due to finite retry limits. The frame payload for each packet is considered to be equal. In may be noted that, unlike most wireless communication protocols (as in [13]), in IEEE 802.15.6, a packet is not dropped due to channel access failure. Therefore, $\mathcal{R}$ is symbolically represented as:

$$\begin{aligned} \mathcal{R} = 1 - P_r = 1 - \sum_{i=0}^{7} \sum_{l=0}^{m} b_{i,-1,L_s,l} \\ \Rightarrow \mathcal{R} = 1 - \beta^{(m+1)(L_c - L_a)} \times b_{0,0,0,0}, \end{aligned} \tag{44}$$

where, P_r is the probability that a packet is dropped due to finite retry limits.

6.2 Throughput

The *throughput* $\mathcal{S}_i$ of a node operating in $UP(i)$ (in bits/second) is defined as the number of bits successfully transmitted over the channel in unit time. Mathematically, for a node operating in $UP(i)$, throughput is defined as the product of the average length of the packets transmitted ($\mathcal{L}$) (in bits), the reliability of the system ($\mathcal{R}$), and the transmission probability (τ_i) of the node. $\mathcal{S}$ can be defined as:

$$\mathcal{S}_i = \mathcal{L} \times \mathcal{R} \times \tau_i, \tag{45}$$

where, $\mathcal{L}$ denotes the average length of the transmitted packets (header length + payload) in bits. Substituting the values of $\mathcal{R}$, and τ_i from Equations (44) and (42) in Equation (45), we obtain the expression for $\mathcal{S}_i$.

6.3 Average Delay

Delay of a received packet is defined as the time interval from the time-instant, when for the first time, a packet moves to the head of the MAC queue and ready to be transmitted, till the I-ACK frame for the transmitted data-packet is received. However, delay corresponding to a packet which is dropped due to finite retry limits, is not taken into consideration. The average delay includes the total time elapsed while a node decrements its backoff counter value (until it reaches zero) in each of the backoff stages and the wait duration for the I-ACK frame. The average delay ($\mathbb{D}$) can be expressed as,

$$\mathbb{D} = \mathfrak{D}_{cu} + T_{fr} + T_{I-ACK} + 2T_p + T_{pr} + 3pSIFS, \tag{46}$$

where $\mathfrak{D}_{cu}$ denotes the average cumulative delay caused by the backoff counter decrements over all the previous backoff stages (for unsuccessful packet transmissions), and the present backoff stage. T_{fr}, T_{I-ACK}, T_p, and T_{pr} denote the average data-frame transmission time, the I-ACK frame transmission time, the frame propagation time, and the average frame processing time, respectively.

6.4 Power Consumption

One of the most important performance parameters is the average *power consumption* for the individual body sensor nodes, as the average lifetime of the WBAN can be estimated by using this parameter. For a sensor node, the In this work, we calculate the average energy consumption (E_t) for a sensor node is computed as,

$$E_t = (\overline{m} - 1)\mathfrak{D}_{cu} \times E_{idle} + (\overline{m})L_s \times E_{tx} + E_{rx}(\overline{m} \times \mathbb{D}), \tag{47}$$

where $\overline{m}$ denotes the average number of backoff stages or retransmission required for successful packet delivery and E_{idle}, E_{tx}, and E_{rx} denote energy consumption in idle state, transmitting state, and receiving state of a node, respectively.

7 Performance Analysis

In this section, we analyze the performance of the IEEE 802.15.6 CSMA/CA protocol under saturated traffic regime for non-ideal channel conditions. Based on the DTMC, we evaluate the performance in terms of reliability, throughput, average delay, and power consumption for a body sensor node. We also compare and contrast the variation of the performance metrics under non-ideal channel conditions against that under ideal channel conditions [24]. Although, in Section 6, we have derived the expressions for performance metrics through accurate analysis of the model, in a practical environment, it may be required for a sensor node to compute internally the values of these parameters as a part of some optimization problem. Therefore, it is required

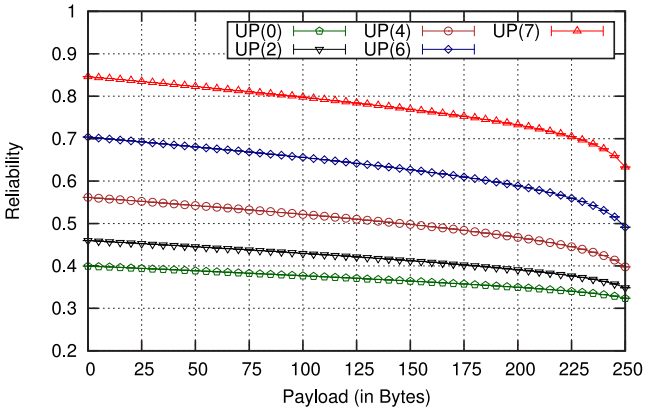

Fig. 4. Reliability versus Payload for different UPs.

to have the simplified forms of these complex non-linear equations by proper approximation.

In order to approximate the expressions for the performance metrics, we first approximate the expression for $b_{0,0,0,0}$, as given by Equation (31). Firstly, we consider the value of β to be considerably small, and, thus, we approximate it as:

$$\frac{1-\beta^m}{1-\beta} \approx 1-\beta, \text{ where } \beta > 0. \tag{48}$$

Also, as per the IEEE 802.15.6 standard, the maximum retry limit for a packet, $m = 7$. Therefore, considering the small magnitude of β, the higher order terms are neglected.

7.1 Simulation Settings

The simulations are performed for a WBAN with 10 sensors and a hub, communicating using the 2.4 GHz ISM band. We have varied the size of payload from 0 to 255 bytes and measured the respective values of different performance parameters. The performance parameters viz. reliability, throughput, average delay, and power consumption are simulated against the frame payload size. The system parameters [32] used for simulation, are given in Table 2.

7.2 Analysis of Reliability

The variation of reliability with the frame payload for different user priorities is shown in Fig. 4. It is noted that with the increase in the frame payload the reliability of the frame transmission decreases for all the user priorities. We also observe that reliability is highest for $UP(7)$, and reliability for all the user priority decreases along with the decrease of the user priority. For the constant payload, the reliability of a node operating in $UP(0)$ is noted to be lowest, and the value is observed to increase as the user priority increases attaining the maximum in case of $UP(7)$. This variation can be explained from the perspective of the contention window size. As the minimum and maximum size (as well as the range) of the contention window gradually increases from $UP(0)$ to $UP(7)$ (see Table 1), the value of the backoff counter chosen by a node is probabilistic large in case of lower user priorities. This increases the probability of unsuccessful packet delivery, which, in turn, reduces the reliability of lower UP nodes.

7.3 Analysis of Throughput

The variation of throughput for all the user priorities against different information data-rates of 971.4 Kbps (2,360-2,400 MHz), 728.6 Kbps (950-958 MHz), and 607.1 Kbps (950-958 MHz) are shown in Figs. 5 and 6. From both the figures it is observed that as the user priority increases, throughput of the node becomes higher. It is concluded that as the value of CW_{min} decreases with the increase of the user priority, the delay is minimized, which in turn, results in transmission of higher number of bit transmission over the channel in unit time duration. It is also observed that for any given user priority, throughput increases almost linearly with the increase of the data rate. The bandwidth efficiency is found to be maximum for $UP(7)$ which then decreases gradually till $UP(0)$.

Moreover, comparing Figs. 5 and 6, we observe that for non-ideal channel conditions, throughput is lower than that for ideal channel conditions. From the expression for throughput, we discern the direct proportionality of reliability with throughput. Hence, we remark that in IEEE 802.15.6 CSMA/CA protocol, the body-sensors operating in higher user priorities can transfer the sensed data to the LDPU more reliably and with higher throughput.

7.4 Analysis of Average Delay

From the expression for delay we observe that it is independent of information data-rate. We illustrate the variation of the expected average delay for both ideal and error-prone channel conditions in Figs. 7a and 7b. It is observed that as the frame payload increases, the expected average delay corresponding to a node increases linearly. Higher frame payload size corresponds to higher frame transmission time, which adds to the concerned average delay factor. Also, we notice that for lower user priorities, i.e., for user priorities with higher value of CW_{min}, the expected average

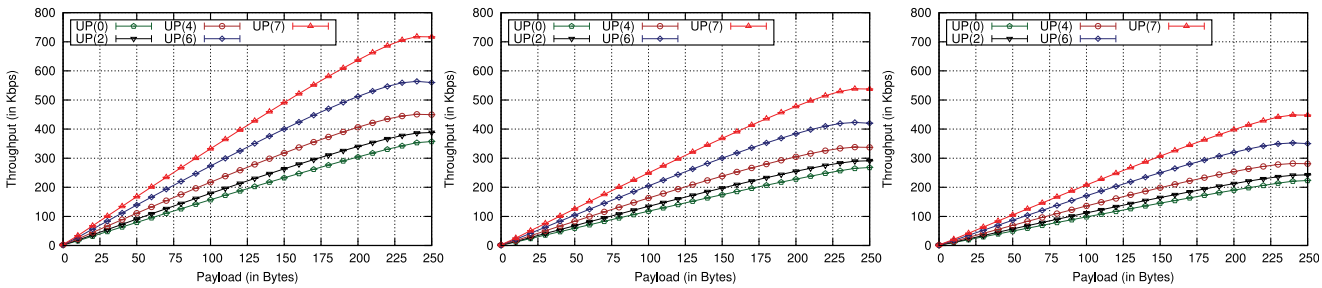

(a) Data rate = 971.4 Kbps (b) Data rate = 728.6 Kbps (c) Data rate = 607.1 Kbps

Fig. 5. Throughput versus Payload for different data rates for ideal channel conditions.

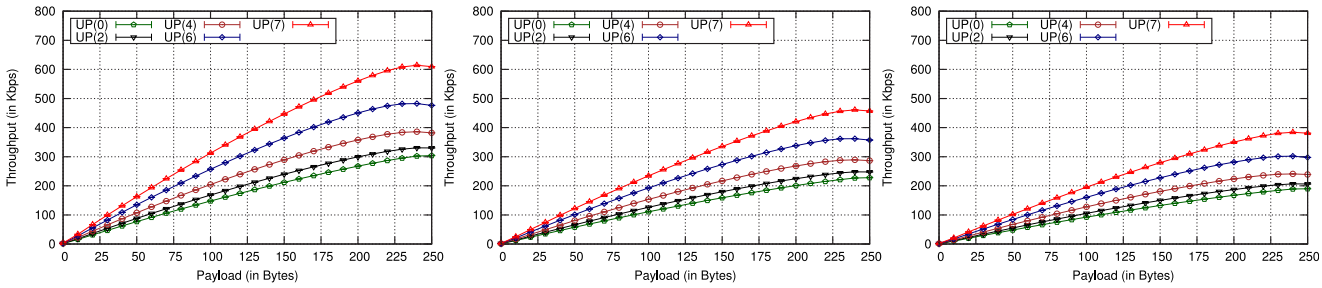

(a) Data rate = 971.4 Kbps (b) Data rate = 728.6 Kbps (c) Data rate = 607.1 Kbps

Fig. 6. Throughput versus Payload for different data rates for non-ideal channel conditions.

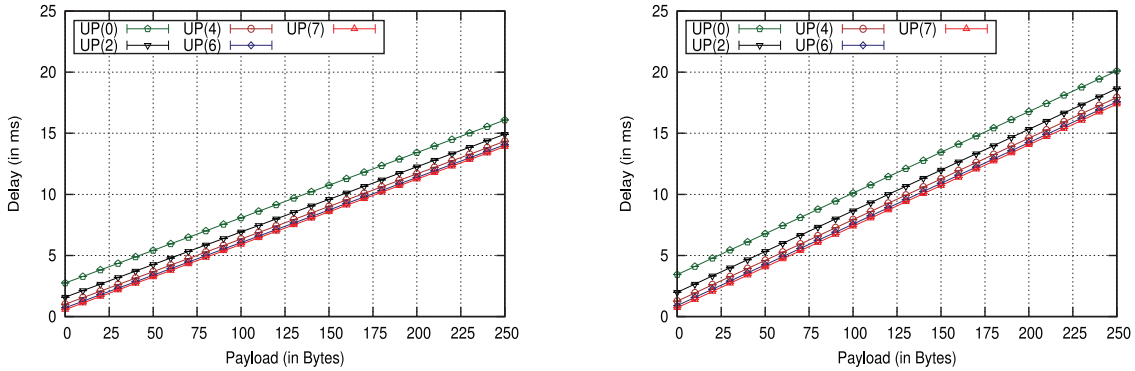

(a) Average delay vs Payload for ideal channel conditions (b) Average delay vs Payload for non-ideal channel conditions

Fig. 7. Average delay versus Payload for different channel conditions.

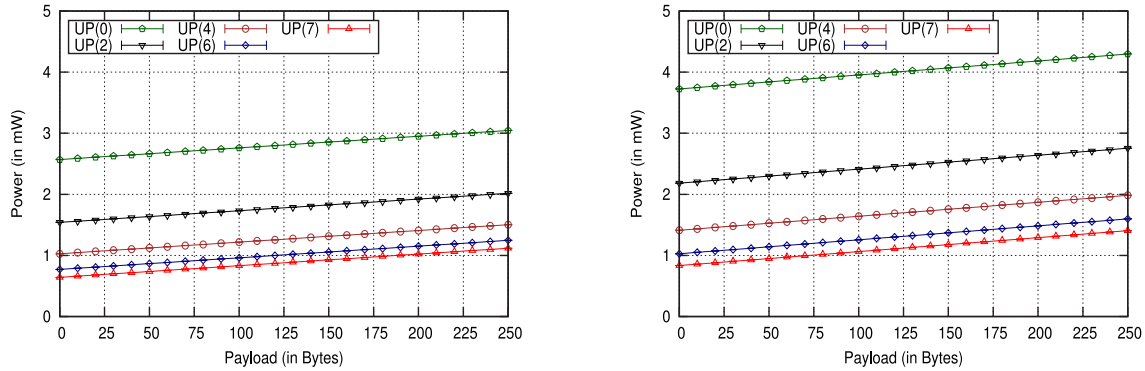

(a) Power consumption vs Payload for ideal channel conditions (b) Power consumption vs Payload for non-ideal channel conditions

Fig. 8. Power consumption versus Payload for different channel conditions.

delay is maximum. As for lower user priority nodes, the size of the backoff counter value is chosen from a greater range, the cumulative expected delay caused by all the backoff counters of different backoff stages is higher than that of a node of higher user priority.

Comparing the two figures (Figs. 7a and 7b), we descend to the fact that for any given user priority and frame payload value, the average expected delay for non-ideal channel conditions is higher than that for ideal channel conditions. For non-ideal channel conditions, the event of unsuccessful packet delivery is driven by the BER. Higher BER associated with the transmission channel corresponds to higher packet drop probability, which indicates the packet will have to be re-transmitted in the following (incremented) backoff stage unless the maximum backoff stage limit is reached. Due to this reason, the average backoff stage at which a packet is successfully transmitted for non-ideal channel conditions has a higher value compared to that for ideal channel conditions.

7.5 Analysis of Power Consumption

Finally, we vary the frame payload to observe its impact on the power consumption of the sensor node. As shown in Figs. 8a and 8b, power consumption is a monotonically increasing parameter with respect to the frame payload size. Higher frame payload size corresponds to higher amount of energy exhausted in transmission of the data-frame. Also, it is observed that power consumption for is minimum $UP(7)$, and it increases proportionately with the value of CW_{min} for the different user priorities,

eventually attaining the maximum at $UP(0)$. As expressed in Equation (47), power consumption is directly proportional to the average delay in transmission for a node. Therefore, it comes as a straightforward deduction that as the average delay is high for lower user priority nodes, the idle state power consumption for the node increases which eventually contributes towards a higher value of power consumption.

Additionally, we also note that for a given user priority and frame payload length, the power consumption for a node operating under non-ideal channel characteristics is higher than that of of a node which operates under ideal channel conditions. For non-ideal channel conditions, due to higher BER, the average backoff stage at which successful transmission of a packet takes place has an expected higher value than that for an ideal channel. This results in a higher magnitude of $\overline{m}$ as expressed in Equation (47), due to which E_t has a higher value for non-ideal channel conditions.

Finally, we observe that in all these results the pair-wise plots for user priorities 0 and 1, 2 and 3, and 4 and 5, respectively, are overlapping to one another in nature. This is a straightforward impact of the identical pair-wise values of the CW_{min} which are proposed in the IEEE 802.15.6 standard. Therefore, it is fair to remark that as the pair-wise results, as mentioned above, do not vary much in term of any of the performance metrics, five user priorities would have been adequate instead of eight. Also, for $UP(7)$, reliability and throughput are noted to maximum, and average delay and power consumption are observed to be minimum. This illustrates the user priority, which is designated for emergency and medical event related traffic, is separated from the remaining user priorities. From a medical scientific perspective, it is highly important, it stands out as one of the prime features which distinguishes this wireless communication standard from the previous ones.

8 Conclusion

This work focuses on the design of a DTMC for modeling the working of the IEEE 802.15.6 CSMA/CA protocol. The model concerns immediate acknowledgement policy under non-ideal channel conditions, and saturated network traffic regime. Unlike the previous related works, we take into consideration the waiting state of a node after the transmission of a data-packet, and, thus, provide an accurate model of the standard. Based on this model, we obtain the expressions for the different performance parameters, and analyze their variation against variede frame payloads. It is concluded, through the analysis, that instead of eight different user priorities, five would have been sufficient. Also, the importance of this new wireless communication standard is realized through comparison of the results of $UP(6)$ and $UP(7)$ (user priorities for high priority emergency and medical event reporting) against the same of the other non-medical user priorities.

In the future, this work can be extended to analyze the performance of the IEEE 802.15.6 slotted CSMA/CA protocol for both ideal and non-ideal channel conditions, saturated and unsaturated traffic regime, and for different acknowledgement policies. Similar research areas can be explored for the IEEE 802.15.6 slotted ALOHA protocol. Also, we would like to quantify the transmission delay and backoff counter frozen duration for the nodes operating under different user priorities, and analyze its impact on a WBAN comprising of a high number of component sensor nodes.

Acknowledgments

Sudip Misra is the corresponding author. A preliminary version of this work is accepted for presentation in IEEE GLOBECOM 2014, Austin, Texas (December 8-12, 2014).

References

[1] I. F. Akyildiz, W. Su, Y. Sankarasubramaniam, and E. Cayirci, "Wireless sensor networks: A survey," *J. Comput. Netw.*, vol. 38, pp. 393–422, 2002.

[2] P. Nicopolitidis, G. I. Papadimitriou, A. S. Pomportsis, P. Sarigiannidis, and M. S. Obaidat, "Adaptive wireless networks using learning automata," *IEEE Wireless Commun.*, vol. 18, no. 2, pp. 75–81, Apr. 2011.

[3] S. Misra and S. Chatterjee, "Social choice considerations in cloud-assisted WBAN architecture for post-disaster healthcare: Data aggregation and channelization," *Inform. Sci.*, vol. 284, pp. 95–117, 2014.

[4] J. Corchado, J. Bajo, D. Tapia, and A. Abraham, "Using heterogeneous wireless sensor networks in a telemonitoring system for healthcare," *IEEE Trans. Inf. Technol. Biomed.*, vol. 14, no. 2, pp. 234–240, Mar. 2010.

[5] S. Misra and S. Sarkar, "Priority-based time-slot allocation in wireless body area networks during medical emergency situations: An evolutionary game theoretic perspective," *IEEE J. Biomed. Health Informat.*, 2014(accepted).

[6] A. B. Waluyo, W.-S. Yeoh, I. Pek, Y. Yong, and X. Chen, "Mobisense: Mobile body sensor network for ambulatory monitoring," *ACM Trans. Embedded Comput. Sys.*, vol. 10, pp. 13:1–13:30, Aug. 2010.

[7] R. Cooper, S. Fitzgerald, M. Boninger, D. Brienza, N. Shapcott, R. Cooper, and K. Flood, "Telerehabilitation: Expanding access to rehabilitation expertise," *Proc. IEEE*, vol. 89, no. 8, pp. 1174–1193, Aug. 2001.

[8] J. Ko, C. Lu, M. Srivastava, J. Stankovic, A. Terzis, and M. Welsh, "Wireless sensor networks for healthcare," *Proc. IEEE*, vol. 98, no. 11, pp. 1947–1960, Nov. 2010.

[9] S. Moulik, S. Misra, C. Chakraborty, and M. S. Obaidat, "Prioritized payload tuning mechanism for wireless body area network-based healthcare systems," in *Proc. IEEE GLOBECOM*, 2014 (accepted).

[10] M. Chen, S. Gonzalez, A. Vasilakos, H. Cao, and V. C. M. Leung, "Body area networks: A survey," *J. Mobile Comput. Appl.*, vol. 16, pp. 171–193, Apr. 2011.

[11] *IEEE Standard for Local and Metropolitan Area Networks—Part 15.6: Wireless Body Area Networks*, IEEE Std., Feb. 2012.

[12] B. Latré, B. Braem, I. Moerman, C. Blondia, and P. Demeester, "A survey on wireless body area networks," *Wireless Netw.*, vol. 17, no. 1, pp. 1–18, 2011.

[13] *IEEE Standard for Local and Metropolitan Area Networks—Part 15.4: Low-Rate Personal Area Networks (LR-WPANs)*, IEEE Std., Sep. 2011.

[14] Q. Pang, S. C. Liew, J. Y. B. Lee, and V. C. M. Leung, "Performance evaluation of an adaptive backoff scheme for WLAN," *Wireless Commun. Mobile Comput.*, vol. 4, pp. 867–879, 2004.

[15] K. S. Kwak, S. Ullah, and N. Ullah, "An overview of IEEE 802.15.6 standard," in *Proc. 3rd Int. Symp. Appl. Sci. Biomed. Commun. Technol.*, Nov. 2011, pp. 1–6.

[16] S. Rashwand and J. Misic, "Performance evaluation of IEEE 802.15.6 under non-saturation condition," in *Proc. IEEE GLOBECOM*, 2011, pp. 1–6.

[17] S. Rashwand, J. Misic, and H. Khazaei, "Performance analysis of IEEE 802.15.6 under saturation condition and error-prone channel," in *Proc. IEEE Wireless Commun. Netw. Conf.*, Mar. 2011, pp. 1167–1172.

[18] S. Rashwand, J. Misic, and H. Khazaei, "IEEE 802.15.6 under saturation: Some problems to be expected," *J. Commun. Netw.*, vol. 13, no. 2, pp. 142–148, Apr. 2011.

[19] S. Rashwand and J. Misic, "Effects of access phases lengths on performance of IEEE 802.15.6 CSMA/CA," *Comput. Netw.*, vol. 56, no. 12, pp. 2832–2846, Aug. 2012.
[20] S. Ullah and K. S. Kwak, "Throughput and delay limits of IEEE 802.15.6," in *Proc. IEEE Wireless Commun. Netw. Conf.*, Mar. 2011, pp. 174–178.
[21] S. Ullah, M. Chen, and K. S. Kwak, "Throughput and delay analysis of IEEE 802.15.6-based CSMA/CA protocol," *J. Med. Syst.*, vol. 36, pp. 3875–3891, May 2012.
[22] G. Bianchi, "IEEE 802.11—Saturation throughput analysis," *IEEE Commun. Lett.*, vol. 2, no. 12, pp. 318–320, Dec. 1998.
[23] G. Bianchi, "Performance analysis of the IEEE 802.11 distributed coordination function," *IEEE J. Sel. Areas Commun.*, vol. 18, no. 3, pp. 535–547, Mar. 2000.
[24] S. Sarkar, S. Misra, C. Chakraborty, and M. S. Obaidat, "Analysis of reliability and throughput under saturation condition of IEEE 802.15.6 CSMA/CA for wireless body area networks," in *Proc. IEEE GLOBECOM*, 2014 (accepted).
[25] *IEEE 802.11-2012 (Revision of IEEE Std 802.11-2007)*, IEEE Std., Mar. 2012.
[26] A. Ahuja, P. V. Krishna, and V. Saritha, "Analysis of a refined model for the IEEE 802.11 distributed coordination function," *Int. J. Commun. Netw. Distrib. Syst.*, vol. 10, no. 1, pp. 66–82, Nov 2013.
[27] P. Park, P. D. Marco, P. Soldati, C. Fischione, and K. H. Johansson, "A generalized Markov chain model for effective analysis of slotted IEEE 802.15.4," in *Proc. IEEE 6th Int. Conf. Mobile Adhoc Sensor Syst.*, Oct. 2009, pp. 130–139.
[28] P. D. Marco, P. Park, C. Fischione, and K. H. Johansson, "Analytical modeling of multi-hop IEEE 802.15.4 networks," *IEEE Trans. Veh. Technol.*, vol. 61, no. 7, pp. 3191–3208, Sep. 2012.
[29] C. Tachtatzis, F. Di Franco, D. Tracey, N. Timmons, and J. Morrison, "An energy analysis of IEEE 802.15.6 scheduled access modes," in *Proc. IEEE GLOBECOM Workshops*, Dec. 2010, pp. 1270–1275.
[30] M. Hernandez, *Body Area Networks Using IEEE 802.15.6: Implementing the Ultra Wideband Physical Layer*, 1st ed., L. Mucchi, Ed. San Francisco, CA, USA: Academic, 2014.
[31] R. Chavez-Santiago, K. Sayrafian-Pour, A. Khalegi, K. Takizawa, J. Wang, I. Balasingham, and L. Huan-Bang, "Propagation models for IEEE 802.15.6 standardization of implant communication in body area networks," *IEEE Commun. Mag.*, vol. 51, no. 8, pp. 80–87, Aug. 2013.
[32] B. H. Jung, R. Akbar, and D. K. Sung, "Throughput, energy consumption, and energy efficiency of IEEE 802.15.6 body area network (BAN) MAC protocol," in *Proc. IEEE 23rd Int. Symp. Pers. Indoor Mobile Radio Commun.*, Sep. 2012, pp. 584–589.

Subhadeep Sarkar is a Ph.D. student in the School of Medical Science and Technology, and a senior research fellow at the School of Information Technology, Indian Institute of Technology Kharagpur. His research interests include wireless body area networks, sensor networks, and cloud computing. Sarkar is a B.Tech. in Computer Science and Engineering.

Sudip Misra is an associate professor in the School of Information Technology at the Indian Institute of Technology Kharagpur. His research interests include wireless sensor networks, wireless body area networks, cloud computing, smart grid, and nano-bio sensor networks. Misra has a Ph.D. in Computer Science from Carleton University, Ottawa.

Bitan Bandyopadhyay is an undergraduate student, currently pursuing his B.E. in Electronics and Telecommunication Engineering, Jadavpur University, India. His research interests include wireless sensor networks, wireless body area networks, and ad hoc networks.

Chandan Chakraborty is an associate professor at the School of Medical Science and Technology, Indian Institute of Technology Kharagpur. He has also received his Ph.D. degree from IIT Kharagpur. His major fields of interest are biostatistics & medical informatics, pattern recognition for medical imaging, quantitative microscopy, computational pathology, and computer aided diagnosis.

Mohammad S. Obaidat received the Ph.D. and M. S. degrees in computer engineering from The Ohio State University, Columbus, Ohio, USA. He is currently a Full Professor in computer science and software engineering with Monmouth University, NJ, USA. He has published about 30 books and 600 refereed technical articles.